Fracture behavior of Lennard-Jones glasses

Christian D. Lorenz* and Mark J. Stevens†
Sandia National Laboratory, Albuquerque, New Mexico 87185, USA
(Received 22 April 2003; published 13 August 2003)

The fracture behavior of binary Lennard-Jones (LJ) glasses is studied by extensive molecular dynamics simulations. These LJ glasses represent a nonbond limit of polymer network glasses. We determine that the low strain behavior of the LJ and polymer glasses is similar. Two different LJ glasses are fractured under tensile strain without any preexisting crack. Void formation and resulting growth as strain increases is the mechanism through which the system fails. Void formation initiates at the yield strain of $\varepsilon_y \simeq 0.09$, which is approximately the same strain at which the yielding behavior is first observed in cross-linked network models of polymer adhesives. The yield stress increased only by small amounts with increased strain rate and with increased system size (from $N = 30\,000$ atoms to 120 000 atoms). Within the ranges tested, the stress-strain behavior of these systems is independent of the temperature drop during quench and the initial molecular configuration.

DOI: 10.1103/PhysRevE.68.021802 PACS number(s): 82.35.−x, 83.60.−a

I. INTRODUCTION

The fracture behavior of materials has been the focus of a large amount of research. Large-scale molecular simulation techniques have become an important tool in investigating material fracture behavior. One of our aims has been to better understand the fracture behavior of highly cross-linked polymer networks, such as epoxies [1,2]. Naturally, there is much interest in understanding the mechanical response of adhesives when a strain is applied to them [3–12].

Epoxy adhesives are highly cross-linked polymer networks. Epoxies are created by curing a liquid mixture of two molecules: a resin and a cross linker. The strands between cross linkers are rather short. A model of epoxies follows that of other coarse-grained polymer models [13,14]. Lennard-Jones (LJ) beads represent groups of a few atoms along the backbone, and are bound together with a simple spring potential. In the epoxy model [1,2], the network has functionality six and just two beads between the cross links, because the strands in epoxy adhesives are short. The amorphous structure occurs because the curing yields a randomly connected network. The coarse-grained, bead-spring model of epoxies [1,2] has been used to simulate the fracture behavior of epoxy systems. The stress-strain behavior of the epoxy systems (Fig. 1) exhibits a yield stress at a strain of $\varepsilon_y \simeq 0.1$, followed by a region of nearly constant stress where the chains are being pulled taut and a region of increasing stress, while bonds are being stretched and broken until finally failure occurs. Here, we investigate what happens if the amorphous structure is not bonded into a network. The objective of this work is to confirm our expectation that the yield behavior at low strains of these highly cross-linked polymer networks will be similar to that of monomeric amorphous systems without cross links or bonds, since the bonds are not stressed at low strains.

In this paper, we present fracture simulations of simple, binary LJ glasses in three dimensions. We study binary LJ glasses since these systems are examples of commonly studied glasses and we expect our result not to depend on the details of the system. These binary LJ systems have also been repeatedly used to model metallic glasses. The early simulation studies [15–21], which focused on the transformation that the system experienced and the dislocations of the atoms when a shear was exerted on it, laid the foundation for understanding the stress-strain behavior of metallic glass systems. Much of the more recent works have used two-dimensional systems to study the physics of crack propagation [22–25] within the glass, where the materials are subjected to very high stresses and undergo large strains. Other molecular simulations of fracture in monomeric LJ materials have been focused on crystalline systems [26–29]. In our case, these LJ glasses allow us to simulate an amorphous system that represents the nonbonded limit of more complex models used to study polymer adhesives. Also, since these binary LJ glasses have been used to model metallic glasses, this work should also be of a more general interest.

In the simulations of the model epoxy system, the tensile stress-strain curve (Fig. 1) shows yielding behavior at a strain of $\varepsilon_y \simeq 0.1$, which evidence suggests is related to the

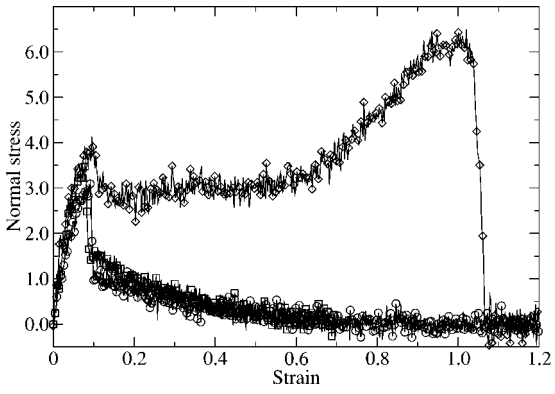

FIG. 1. Comparison of the stress-strain behavior of system I (○) and system II (□) mixtures of monomers, when a strain rate of $3.1\times10^{-5}\tau^{-1}$ is applied to each system. A typical stress-strain behavior of a highly cross-linked epoxy system (from Ref. [1]) is also shown (◇).

*Electronic address: cdloren@sandia.gov
†Electronic address: msteve@sandia.gov

strain required to separate the nearest neighbor LJ beads [1,2]. Bonds are not stretched at this strain. Baljon and Robbins [12] have investigated the crazing and fracture behavior of polymer adhesives using a similar coarse-grained model with no cross linking. They found stress-strain behavior at low strain similar to that observed in the model epoxy systems. Specifically, they observed that the stress would peak at very low strains, as observed in the cross-linked systems, and then the stress would plateau and then decay to zero. They found that the yield strain is independent of the polymer chain length used in the system, but the decay to zero stress slowed as the polymer chain length increased.

In the case of LJ atomic glasses, we expect to see that the stress-strain behavior will follow a similar trend as observed by Baljon and Robbins [12] for adhesive systems as the polymer chain size was decreased. At low strain, we expect the yield strain to occur at $\varepsilon \simeq 0.1$, because at that strain the LJ beads making up the atomic glass would be separated from their nearest neighbors. We expect to see a rapid decay to zero stress, upon further increase in the strain, corresponding to the continual separation of particles (void formation), until fracture occurs. Our simulation results presented in Sec. III confirm these expectations.

In the following sections of this paper, we present the work done to understand how the stress-strain behavior of three-dimensional binary LJ systems depends on strain rate, quench rate, and equilibration times. The following section introduces the two systems that are studied and our simulation method. Then we will present and discuss the results from these simulations.

II. SIMULATION METHODS

The particles in the binary systems interact solely through the LJ potential [30]:

$$U_{\mathrm{LJ}}(r) = 4u_0\left[\left(\frac{d}{r}\right)^{12} - \left(\frac{d}{r}\right)^{6}\right], \tag{1}$$

where d and u_0 have been used to represent the LJ diameter and the LJ energy, respectively. Traditionally, the symbols "σ" and "ε" are used to represent the LJ diameter and energy, but in this paper they are being used for stress σ and strain ε. The two different systems each consisted of an 80/20 mixture of particle *A* to particle *B*. These binary mixtures allowed us to form amorphous systems, as opposed to crystalline structures which result when using monatomic LJ systems. The LJ parameters that were used in both systems are shown in Table I. For both systems, the cutoff for the LJ potential has been set to $2.5d$.

The LJ parameters of system I binary mixture was first used by Ernst *et al.* [31]. The system II parameter set was first used by Kob and Andersen in 1994 [32]. Weber and Stillinger had used a similar potential for their simulations of $Ni_{80}P_{20}$ [33]. Since these initial studies, many other authors have employed this parameter set in their studies of metallic glasses [34–40].

In the *z* dimension, the system is bounded between two rigid walls, which consist of particles arranged in two (111) layers of the fcc lattice structure such that the nearest-neighbor distance is $1.204d$. The system is periodic in the *x* and *y* dimensions. The particles interact with wall particles *W* as governed by the LJ potential (Table I); however, the wall particles do not interact with one another.

TABLE I. Lennard-Jones parameters used to define the interaction between particles *A* and *B* and the wall particles *W* in the two systems (I and II).

Interaction pair	u_0 (I)	u_0 (II)	d (I)	d (II)
AA	1.0	1.0	1.0	1.0
AB	1.0	1.5	0.9	0.8
BB	1.0	0.5	0.8	0.88
AW, *BW*	1.0	1.0	1.0	1.0

The glass formation and strain simulations were conducted on the computational plant [41] at Sandia National Laboratories using LAMMPS [42], which is a massively parallel molecular dynamics (MD) code. The average run for a 60 000 bead system took about 4 000 node hours (approximately 5 days on 32 nodes). The temperature of the system was controlled by the Langevin thermostat [43] with a Langevin damping constant of $1.0\tau^{-1}$ and an integration time step of 0.005τ, where τ is the LJ time unit.

The majority of the work presented in this paper studied systems of 60 000 particles in a rectangular box. The system size effects were studied by conducting simulations of system I with 30 000 and 120 000 particles. In all the cases, the systems were sized such that the liquid density $\rho_{\diagup}$ would be consistent with the liquid temperature $T_{\diagup}$. For most of our studies, $T_{\diagup} = 1.1\ u_0/k_B$ and systems were sized so that system I liquid density is 0.9 ($50.0d \times 33.7d \times 48.3d$ for 60 000 particles) and the system II liquid density is 0.8 ($45.8d \times 36.1d \times 44.1d$ for 60 000 particles).

These simulations follow the same basic approach as in the earlier epoxy simulations [1,2]. The particles are initially placed randomly allowing overlap. Overlap is removed by applying a cosine potential

$$U_{\mathrm{soft}} = A + A\cos\left(\frac{\pi r}{r_0}\right), \tag{2}$$

where $r_0 = 2^{1/6}d$ is the cutoff. The amplitude *A* is increased from 0.0 to 60.0 over the span of 5000 time steps to separate the overlapping particles. Then the system is equilibrated at $T_{\diagup} = 1.1\ u_0/k_B$ and $\rho_{\diagup}(T_{\diagup})$ for 10 000 time steps to remove artifacts of the initial state.

After the equilibration of the liquid state, the system is quenched to a temperature $T = 0.2\ u_0/k_B$, which is well below the systems' glass transition temperature of $T_g \simeq 0.40u_0/k_B$ [31] and $T_g \simeq 0.435u_0/k_B$ [32], for systems I and II, respectively. In order to allow the density to increase due to the quench, the top wall is allowed to move rigidly under a small pressure ($P_{wall} = 0.1u_0/d^3$). After quenching, the walls are held fixed and the system is run at $T = 0.2\ u_0/k_B$ for 100 000 time steps before the application of the tensile strain. The tensile strain is applied by moving the

top wall at a constant velocity, v_z, in the z direction; the bottom wall remains fixed in position. The strain behavior was studied for $v_z = 0.01d/\tau$, $0.001d/\tau$, and $0.0001d/\tau$, which corresponds to strain rates of $\dot{\varepsilon} = 3.1\times10^{-4}\tau^{-1}$, $3.1\times10^{-5}\tau^{-1}$, and $3.1\times10^{-6}\tau^{-1}$, respectively.

To test whether the initial liquid system is sufficiently equilibrated, we compared the stress-strain behavior for system I mixtures that were quenched at different times. By quenching at different times, we are able to sample systems having statistically independent initial configurations. The results from these simulations suggest that the stress-strain behavior is not affected by a change in the initial configuration of the beads. In order to keep the simulation time at a minimum, we equilibrated the liquid systems for the least amount of time steps that we studied (10 000 time steps).

III. RESULTS

Figure 1 shows the stress-strain behavior of both systems for $\dot{\varepsilon} = 3.1\times10^{-5}\tau^{-1}$. Similar behavior is observed for both systems. The stress on the system increases as the strain increases until it reaches a peak at the yield stress σ_y and strain ε_y. The yield stress occurs at almost identical values for system I ($\varepsilon_y \simeq 0.09$, $\sigma_y \simeq 3.0$) and for system II ($\varepsilon_y \simeq 0.07$, $\sigma_y \simeq 3.5$). Similar values of σ_y and ε_y were found in the model cross-linked epoxy simulations [1,2]. In the highly cross-linked systems, no bonds were stretched or broken for $\varepsilon < \varepsilon_y$ so the similarity in the stress-strain behavior is expected.

After the peak, the stress-strain behavior of the monomeric glass systems differs from that of the model epoxy systems. In the monomeric glasses, a brittle fracture behavior is observed in the form of the sharp drop in the stress until $\varepsilon \simeq 0.10$. Other simulation studies [23–25,36,44] of glasses have found that the systems yield at strains in the range of $\varepsilon_y \simeq 0.05-0.10$, which is consistent with our results. Then a more gradual decay in the stress is observed until it reaches zero at $\varepsilon \simeq 0.62$. However, in the model epoxy case, a plateau in the stress follows the peak and then a second peak in the stress is observed, which is then followed by a sharp drop to zero stress as shown in Fig. 1. The stress plateau and second peak are related to the stretching and breaking of bonds in the cross-linked network, which are not expected to be seen in the monomeric glass systems.

As the system is strained, we expect that void formation leads to the yielding of the system, as observed in the model epoxy systems. This expectation is supported by direct observation. As the strain on the system increases from 0 to ε_y, the volume of the system increases nonuniformly. The yield strain corresponds to overcoming the maximum in the LJ force, which is required in order to separate neighboring pairs of beads [1]. The maximum LJ force is exhibited at $r = 2^{1/6}d = 1.12d$, which is the average separation of the beads after a strain of 0.1 is applied to the system.

In order to verify whether voids form at ε_y, we examined images of the system I glass. Figure 2 shows vertical slices, whose thickness is $6d$, of a system I glass, which is being strained at a rate of $\dot{\varepsilon} = 3.1\times10^{-5}\tau^{-1}$. The void is first visible at $\varepsilon = \varepsilon_y \simeq 0.093$. The initial void, which is shown in the middle frame of Fig. 2(a), is $\approx 3\sigma$ in diameter. After the void formation at the stress peak, the void then grows into the bulk of the system, as shown in Figs. 2(b) and 2(c). The void grows very rapidly in the range of strains from the yield strain until $\varepsilon \simeq 0.10$, which is the same strain range over which a sharp drop in the stress is observed. For $\varepsilon > 0.10$, where the strain decays to zero, the void grows at a slower but constant rate until it spans the entire system at $\varepsilon \simeq 0.63$. In all cases, we see the same general void initiation and growth behavior. First, a single void initially forms away from the wall. Then the void grows into the bulk much faster than it grows towards the wall because the particles close to the wall are more close packed and take more energy to separate.

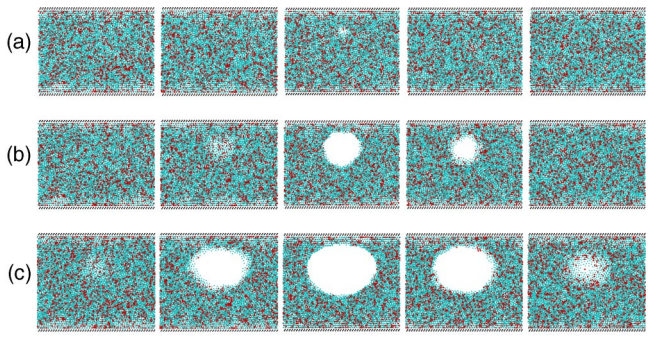

FIG. 2. Void initiation and growth in system I when a strain rate of $3.1\times10^{-5}\ \tau^{-1}$ is applied. Each picture represents a vertical slice of the system which is $6d$ thick. The five slices comprise the whole system. The progression represents increasing the strain from (a) $\varepsilon_y \simeq 0.093$ (the peak in Fig. 4) to (b) $\varepsilon \simeq 0.095$ to (c) $\varepsilon \simeq 0.199$. Although the strain is increasing, the pictures have been rescaled so that they all have the same dimensions. Also, the particles have been imaged with a diameter of $0.5d$.

Holian and Ravelo [45] and Abraham *et al.* [46] have found that in order to accurately study crack propagation in crystalline systems they must use very large systems ($N \sim 10^6$ atoms). Large systems are required so that disturbances emanating from the crack do not have time to reflect from the boundaries and effect the propagation behavior. However, in our amorphous systems, we do not believe that size will have such a large of effect because we are not studying the brittle fracture of the crystalline system. In addition, we are not simulating crack propagation at the crack tip of the material. We are investigating material deformation and crack initiation.

In order to test the system size dependence, systems with $N = 30\,000$, $60\,000$, and $120\,000$ are simulated. Figure 3 shows the stress-strain behavior for system I with different N. (Note: The data are identical for all cases at strains $\varepsilon > 0.2$, so this part of the plots will be excluded in the remaining figures.) There is a small variation in the yield strain, which was determined by interpolating the strain at the midpoint ($\sigma = 2.0$) of the sharp drop in the stress [$\varepsilon_y \simeq 0.091$ ($N = 30\,000$), 0.095 ($N = 60\,000$), 0.102 ($N = 120\,000$)]. The yield strain increases by $0.004-0.007$ as the size of the system is doubled. The larger system allows

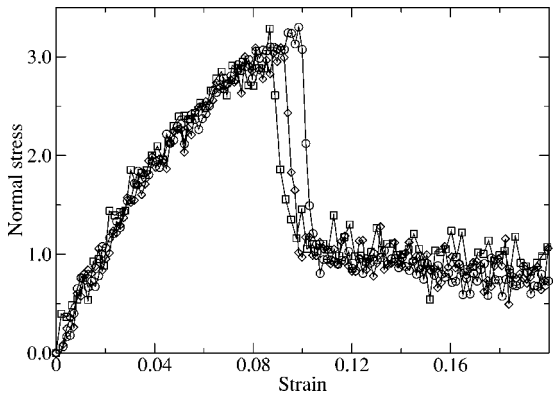

FIG. 3. Plots of the stress-strain behavior of different sized system I, which are being strained at a rate of $\dot{\varepsilon}=3.1\times10^{-5}\ \tau^{-1}$. Each curve represents a different sized system: $N=30\,000$ (□), 60 000 (◇), 120 000 (○) particles.

the strain to be shared over more of the volume. Therefore, a larger strain is required to create the inhomogeneity in the density of the system that results in the formation of a void. At very large N, we expect that the yield strain will reach a constant value, because this size effect will become unnoticeable.

The strain rate was also varied for both systems. Decreasing the strain rate allows the system more time to relax. However, the relaxation of glasses is very slow and polymer glass experiments [47] and simulations [11] have shown a weak dependence ($\varepsilon_y \sim \log v$) of the fracture behavior on the strain rate. Figures 4 and 5 show the stress-strain behavior for system I and system II, respectively, at three strain rates. In both systems, ε_y is weakly dependent on $\dot{\varepsilon}$ [system I: $\varepsilon_y \simeq 0.122$ ($\dot{\varepsilon}=0.000\,31\ 1/\tau$), 0.095 ($\dot{\varepsilon}=0.000\,031\ 1/\tau$), 0.088 ($\dot{\varepsilon}=0.000\,003\,1\ 1/\tau$); system II: $\varepsilon_y \simeq 0.121$ ($\dot{\varepsilon}=0.000\,311/\tau$), 0.088 ($\dot{\varepsilon}=0.000\,031\ 1/\tau$), 0.085 ($\dot{\varepsilon}=0.000\,003\,1\ 1/\tau$)]. The small dependence of the yield strain on the strain rate for both systems supports that these simulations produce results consistent with experiment.

The formation of the glass structure involves a large temperature drop. For comparison, the epoxy systems are generally cured in the liquid state at a temperature around, for example, $T_g=350$ K. Fracture measurements are typically performed at room temperature $T=300$ K, corresponding to a normalized temperature drop of $\Delta T_q=1/6$. In our binary glass simulations, we are limited in how small ΔT_q can be. As T_g approaches T_g, the diffusion of the particles slows down, which results in longer equilibration times that make the length of our simulation unmanageable. We investigated the effect of decreasing ΔT_q on the stress-strain behavior. System I was prepared at different liquid temperatures ($T_g \simeq 0.6$, 0.8, and $1.1u_0/k_B$) and then each was quenched to $T=0.2\ u_0/k_B$, such that the different cases represent $\Delta T_q=2.0$, 3.0, and 4.5. Figure 6 shows that the stress-strain behavior for the different cases is insensitive to the temperature drop during quenching at the given strain rate. While we do not claim that the results we observe at $\Delta T_q=2.0$ are the same as what would be observed at $\Delta T_q=1/6$ (or $\Delta T_q \to 0$), our results suggest that at the given strain rate the yield strain is not sensitive to ΔT_q. Also, we expect that there is a coupling between v_z and ΔT_q, because these two different phenomena occur on different timescales. In the regime of much

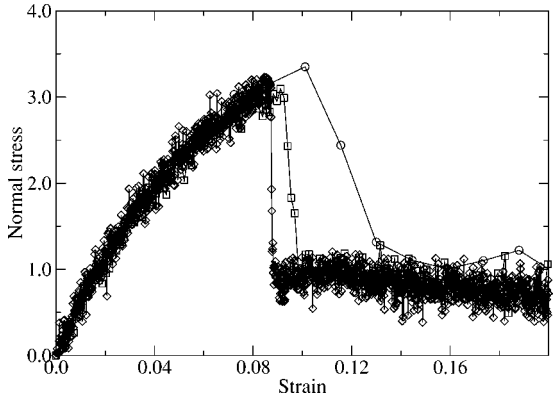

FIG. 4. Comparison of different strain rates on the strain behavior of system I. Each curve represents a different strain rate: $\dot{\varepsilon}=3.1\times10^{-4}\ \tau^{-1}$ (○), $\dot{\varepsilon}=3.1\times10^{-5}\ \tau^{-1}$ (□), and $\dot{\varepsilon}=3.1\times10^{-6}\ \tau^{-1}$ (◇).

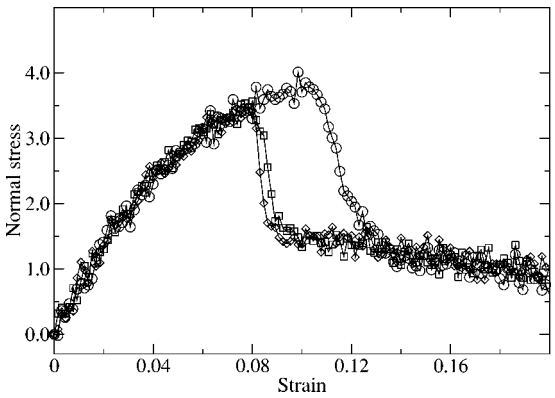

FIG. 5. Comparison of different strain rates on the strain behavior of system II. Each curve represents a different strain rate: $\dot{\varepsilon}=3.1\times10^{-4}\ \tau^{-1}$ (○), $\dot{\varepsilon}=3.1\times10^{-5}\ \tau^{-1}$ (□), and $\dot{\varepsilon}=3.1\times10^{-6}\ \tau^{-1}$ (◇).

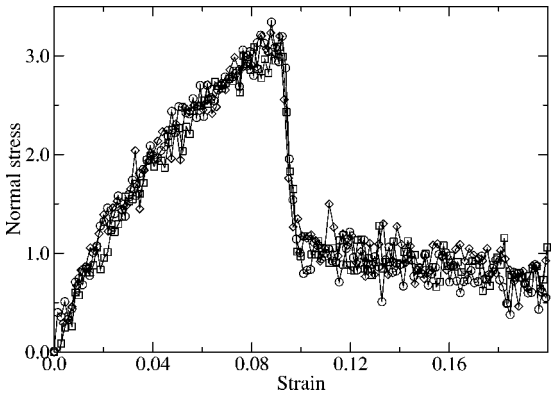

FIG. 6. Plots of the stress-strain behavior of system I samples that experienced a temperature drop of $\Delta T_q=2.0$ (◇), 3.0 (○), and 4.5 (□) during the quench and then were strained at a rate of $\dot{\varepsilon}=3.1\times10^{-5}\ \tau^{-1}$.

slower v_z, which we did not sample, we expect that the yielding behavior will be dependent on ΔT_q.

IV. CONCLUSIONS

The results from three-dimensional MD simulations of binary LJ glasses have been presented in order to provide a better understanding of the stress-strain behavior of these glasses. The correspondence between the deformations and the stress-strain behavior has been characterized. In general, we observed that a void begins to form at the peak in the stress/strain curve. This peak occurs at a yield strain of $\varepsilon_y \simeq 0.09$ which is directly related to the distance required to overcome the LJ particle interaction between nearest neighbors. As the strain increases beyond ε_y, the single void continues to grow until it spans the entire system and fracture occurs. During the growth of the void, we saw that with increasing strain the stress on the system decreases at a rate slower than we expected. This stress-strain behavior is consistent with the behavior observed from other simulations [23–25,36] and experimental [48] studies of the fracture of metallic glasses and polymer systems.

We also investigated how the stress-strain behavior changed as a function of various physical and simulation parameters. The physical parameters that we studied were the strain rate and the temperature drop during quenching ΔT_q. We found that the yield strain ε_y slightly increased with increasing strain rate for both systems. The yield strain ε_y showed no dependence on ΔT_q, within the range that we simulated. The simulation parameters that were varied were the system size and the initial molecular configurations. When the size of the system was increased we found that ε_y increased weakly. Finally, we found that the stress-strain behavior did not change with different initial molecular configurations.

In comparison with the stress-strain behavior of the cross-linked network systems [1,2], we observe similar low strain behavior in the atomic glass systems presented in this paper. As expected, the behavior of the cross-linked and entangled polymer systems [8–10,12] is significantly different for strains larger than ε_y. The plateau observed in both systems and the second peak observed in the cross-linked system are caused by the stretching (or dis-entangling) and subsequent breaking of the bonds, which occur when $\varepsilon > \varepsilon_y$. These results reinforce the previous evidence that the bonds do not influence the stress-strain behavior until larger strains.

ACKNOWLEDGMENT

This work was supported by the U.S. DOE under Contract No. DE-AC04-94AL85000. Sandia is a multiprogram laboratory operated by Sandia Corportation, a Lockheed Martin Company, for the U.S. Department of Energy's National Nuclear Security Administration.

[1] M.J. Stevens, Macromolecules **34**, 2710 (2001).
[2] M.J. Stevens, Macromolecules **34**, 1411 (2001).
[3] A.R. Akisanya and N.A. Fleck, Int. J. Fract. **58**, 93 (1992).
[4] C. Stainton, W. Liang, and K. Kendall, Eng. Fract. Mech. **61**, 83 (1998).
[5] M.S. Kafkalidis, M.D. Thouless, Q.D. Yang, and S.M. Ward, J. Adhes. Sci. Technol. **14**, 1593 (2000).
[6] R.P. Wool, *Polymer Interfaces: Structure and Strength* (Hanser Press, New York, 1995).
[7] A. Kinloch and R. Young, *Fracture Behavior of Polymers* (Applied Science Publishers, London, 1983).
[8] A.R.C. Baljon and M.O. Robbins, Science **271**, 482 (1996).
[9] D. Gersappe and M.O. Robbins, Europhys. Lett. **48**, 140 (1999).
[10] J. Rottler, S. Barsky, and M.O. Robbins, Phys. Rev. Lett. **89**, 148304 (2002).
[11] A.R.C. Baljon and M.O. Robbins, MRS Bull. **22**, 22 (1997).
[12] A.R.C. Baljon and M.O. Robbins, Macromolecules **34**, 4200 (2001).
[13] In *Monte Carlo and Molecular Dynamics Simulations in Polymer Science*, edited by K. Binder (Oxford, New York, 1995).
[14] K. Kremer and G. Grest, in *Monte Carlo and Molecular Dynamics Simulations in Polymer Science* (Ref. [13]), Chap. 4, pp. 194–271.
[15] A. Argon and H. Kuo, Mater. Sci. Eng. **39**, 101 (1979).
[16] A. Argon and L. Shi, Acta Metall. **31**, 4999 (1983).
[17] F. Spaepen, Acta Metall. **25**, 407 (1977).
[18] D. Deng, A.S. Argon, and S. Yip, Philos. Trans. R. Soc. London, Ser. A **329**, 549 (1989).
[19] D. Srolovitz, K. Maeda, V. Vitek, and T. Egami, Philos. Mag. A **44**, 847 (1981).
[20] D. Srolovitz, V. Vitek, and T. Egami, Acta Metall. **31**, 335 (1983).
[21] K. Maeda and S. Takeuchi, Phys. Status Solidi A **49**, 685 (1978).
[22] M.L. Falk, Phys. Rev. B **60**, 7062 (1999).
[23] M.L. Falk and J.S. Langer, Phys. Rev. E **57**, 7192 (1998).
[24] G. Gagnon, J. Patton, and D.J. Lacks, Phys. Rev. E **64**, 051508 (2001).
[25] D.L. Malandro and D.J. Lacks, J. Chem. Phys. **110**, 4593 (1999).
[26] F.F. Abraham, D. Brodbeck, R.A. Rafey, and W.E. Rudge, Phys. Rev. Lett. **73**, 272 (1994).
[27] A. Omeltchenko, J. Yu, R.K. Kalia, and P. Vashishta, Phys. Rev. Lett. **78**, 2148 (1997).
[28] V. Bulatov, F.F. Abraham, L. Kubin, B. Cevindre, and S. Yip, Nature (London) **39**, 669 (1998).
[29] C.L. Rountree, R.K. Kalia, E. Lidorikis, A. Nakano, L. Van Bruntzel, and P. Vashista, Annu. Rev. Mater. Res. **32**, 377 (2002).
[30] M. Allen and D. Tildesley, *Computer Simulation of Liquids* (Clarendon Press, Oxford, 1987).
[31] R.M. Ernst, S.R. Nagel, and G.S. Grest, Phys. Rev. B **43**, 8070 (1991).
[32] W. Kob and H.C. Andersen, Phys. Rev. Lett. **73**, 1376 (1994).
[33] T.A. Weber and F.H. Stillinger, Phys. Rev. B **31**, 1954 (1985).
[34] D.J. Lacks, Phys. Rev. Lett. **87**, 225502 (2001).

[35] T.F. Middleton, J. Hernández-Rojas, P.N. Mortenson, and D.J. Wales, Phys. Rev. B **64**, 184201 (2001).
[36] M. Utz, P.G. Debenedetti, and F.H. Stillinger, Phys. Rev. Lett. **84**, 1471 (2000).
[37] S. Sastry, P.G. Debenedetti, and F.H. Stillinger, Nature (London) **393**, 554 (1998).
[38] T.B. Schroder, S. Sastry, J.C. Dyre, and S.C. Glotzer, J. Chem. Phys. **112**, 9834 (2000).
[39] C. Donati, F. Sciortino, P. Tartaglia, Phys. Rev. Lett. **85**, 1464 (2000).
[40] F. Sciortino, W. Kob, P. Tartaglia, J. Phys.: Condens. Matter **12**, 6525 (2000).
[41] R. Brightwell, L.A. Fisk, D.S. Greenberg, T. Hudson, M. Levenhagen, A.B. Maccabe, and R. Riesen, Parallel Comput. **26**, 243 (2000).
[42] S.J. Plimpton, J. Comput. Phys. **117**, 1 (1995).
[43] J. Schneider, W. Hess, and R. Klein, J. Phys. A **18**, 1221 (1985).
[44] C.F. Fan, Macromolecules **28**, 5215 (1995).
[45] B.L. Holian and R. Ravelo, Phys. Rev. B **51**, 11 275 (1995).
[46] F.F. Abraham, R. Walkup, H. Gao, M. Duchaineau, T.D. De La Rubia, and M. Seager, Proc. Natl. Acad. Sci. U.S.A. **99**, 5777 (2001).
[47] W. Döll, Adv. Polym. Sci. **52**, 105 (1983).
[48] A.L. Greer, Science **267**, 1947 (1995).